Ultrahigh-Energy-Resolution Inelastic X-Ray Scattering Spectroscopy *

E. Burkel

Sektion Physik, University of Munich, Munich, Germany

Z. Naturforsch. **48a**, 289–294 (1993); received January 8, 1992

Very-high-energy-resolution measurements using X-rays can be achieved by extreme backreflection (Bragg angle close to 90°) from perfect crystals. This technique allowed the development of the instrument INELAX for inelastic scattering experiments at the HARWI wiggler at DORIS, DESY Hamburg. Recently, a high energy resolution of 9 meV could be achieved, and the instrument proved to be an excellent tool to investigate collective excitations in condensed matter. Energy transfers from 10 meV to 12 eV and wavevectors up to about 10 $Å^{-1}$ are accessible.

Key words: Inelastic X-ray scattering; Collective excitations; Phonons; Electronic excitations; Zone-boundary collective states.

Since its discovery in 1912 X-ray diffraction has been an extremely successful tool to reveal the local arrangement of atoms and molecules in crystal lattices. In addition, inelastic X-ray scattering based on Compton's observations in 1922 has given information on the electron momentum density. The energy resolution of such inelastic experiments, however, was not sufficient to allow the direct observation of excitations like lattice vibrations. The situation changed with the high intensity of X-rays emitted by synchrotron radiation sources. Meanwhile, very high energy resolution can be obtained by extreme backreflection with Bragg scattering from perfect single crystals at Bragg angles θ close to 90° (backscattering) [1]. This technique allowed the development of the instrument INELAX for inelastic-scattering experiments at the HARWI wiggler at DORIS (HASYLAB, Hamburg) [2, 3] and the direct measurements of lattice vibrations [2–4] and of low-lying electronic excitations [3, 5].

In a Bragg-scattering experiment the energy resolution is limited by the divergence $\delta\theta$ of the beam and the reflection width $\delta\tau$ of the perfect crystal. The energy resolution is given by

$$\frac{\delta E}{E} = \frac{\delta k}{k} = \frac{\delta \tau}{\tau} + \cot\theta \cdot \delta\theta\,, \qquad (1)$$

where $\boldsymbol{k}$ is the wavevector of the radiation and $\boldsymbol{\tau}$ the reciprocal lattice vector. The reflection width $\delta\tau$ is the extension of the reciprocal lattice point parallel to $\boldsymbol{\tau}$. It is essentially proportional to the reciprocal number of the lattice planes involved in the scattering process. Therefore, the first part of (1) describes the intrinsic energy resolution of the crystal in the scattering process. This contribution can be minimized by using perfect crystals, and an energy resolution better than 10 meV can be achieved by using a Si-reflection of the type (hhh), for $h>7$. This is demonstrated by Fig. 1

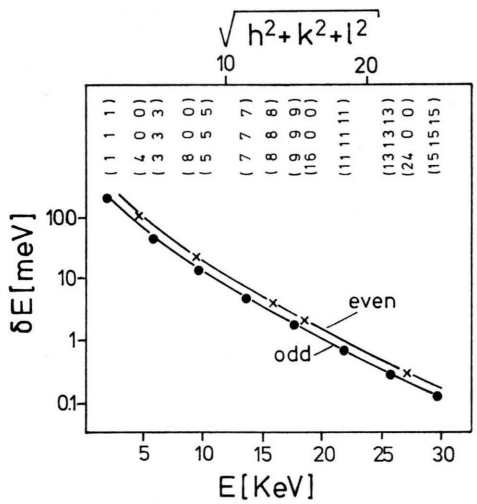

Fig. 1. Intrinsic energy resolution of Si as a function of X-ray energy for different (hhh) and $(h00)$ reflections in backscattering geometry.

* Presented at the Sagamore X Conference on Charge, Spin and Momentum Densities, Konstanz, Fed. Rep. of Germany, September 1–7, 1991.

Reprint requests to Dr. E. Burkel, Sektion Physik der Universität München, Geschwister-Scholl-Platz 1, D-W-8000 München 22, Fed. Rep. of Germany.

0932-0784 / 93 / 0100-0289 $ 01.30/0. – Please order a reprint rather than making your own copy.

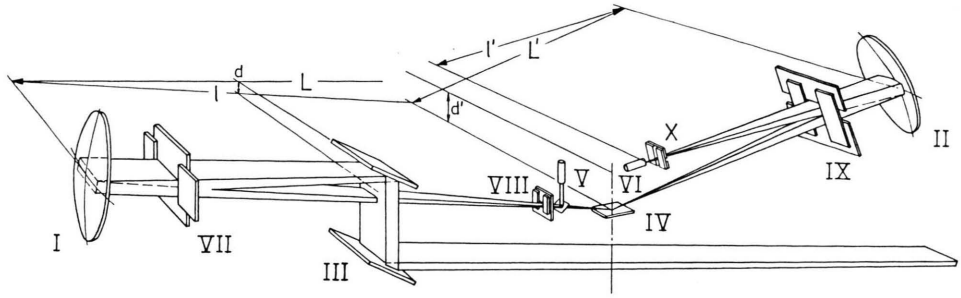

Fig. 2. The instrument INELAX at the HARWI wiggler line of HASYLAB. The beam passes the premonochromator (III) and the monochromator (I) before it illuminates the sample (IV). The scattered intensity is focused by the analyzer (II) into the detector (VI). The primary intensity is controlled by a monitor unit (V). (VII–X) indicate slit systems. For lengths of the labeled distances see Table 1.

showing the intrinsic energy resolution of Si as a function of the photon energy for different (*hhh*) and (*h*00) reflections in backscattering geometry.

According to (1), the second important contribution to the energy resolution arises from the variation of the scattering angle and is, therefore, determined by the geometry of the scattering process.

The inelastic X-ray scattering spectrometer INELAX has been built in several stages since 1984 at the DORIS II storage ring of HASYLAB at DESY, Hamburg. Initially, the spectrometer had been installed at a DORIS beam port using the radiation from a bending magnet. It was later moved to the wiggler line W 2 (HARWI). The latest set-up [3] is shown schematically in Figure 2. The primary parts of the instrument are the monochromator (I) and the analyzer (II) units. Both components consist of spherically bent crystal silicon disks and operate under extreme Bragg backreflection with $\theta = 89.98°$ at the monochromator and $\theta = 89.95°$ at the analyzer. The photon beam from the storage ring passes the premonochromator (III) on its way to the monochromator. This premonochromator acts essentially as a heat filter to protect the monochromator, which defines the desired small energy bandwidth of the photon beam focused onto the sample (IV). The beam intensity is registered by a monitor device (V), using the scattered intensity from a kapton foil within the beam path.

The analyzer crystal collects the radiation scattered by the sample from a variable solid angle and focuses it onto the detector (VI), which is an ion-implanted Si-diode working just below room temperature. Various slit systems (VII–X) help to define the beam cross-section and the scattering geometry and to reject radiation at unwanted energies, arising due to imperfections of the focusing elements. The sample is mounted on a special diffractometer with a horizontal axis and a large detector arm, which serves as a mount for the analyzer unit as well.

Table 1. Geometric distances of INELAX (Fig. 2) at the HARWI wiggler at DORIS. The source for the beam entering the analyzer is slit VIII.

Distances		Monochromator	Analyzer
Source to crystal	L/m	38	2.6
Crystal to image	l/m	8	2.5
Bending radius	R/m	13	2.55
Distance between both beams	d/mm	6	4
Beam size at the crystal	D_{hor}/mm	90	80
	D_{ver}/mm	8	80
Crystal element size	w_{hor}/mm	1	1
	w_{ver}/mm	1	1
Source size	h_{hor}/mm	3.5	2
	h_{ver}/mm	0.5	1

Most of the beam line is enclosed in vacuum tubes to reduce the intensity losses due to absorption along a distance of 51 meters. The relevant geometrical distances of the instrument INELAX are given in Table 1. At present the instrument INELAX is working with the (9 9 9) Bragg reflections of Si at the monochromator and analyzer crystal. Therefore, an initial energy of 17.8 keV is selected. With the scattering angles mentioned above an energy resolution of the instrument of (9.3 ± 1) meV is achievable. This value is obtained by recording the elastically scattered intensity from fused silica as a function of the energy transfer, which is determined by the temperature difference between the analyzer and the monochromator crystals in the technique of INELAX (Figure 3).

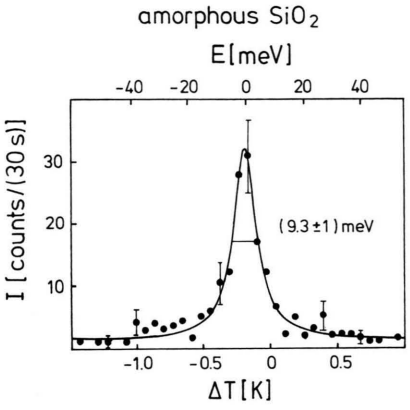

Fig. 3. Intensity, elastically scattered from fused silica, as a function of the temperature difference between monochromator and analyzer and the corresponding energy transfer.

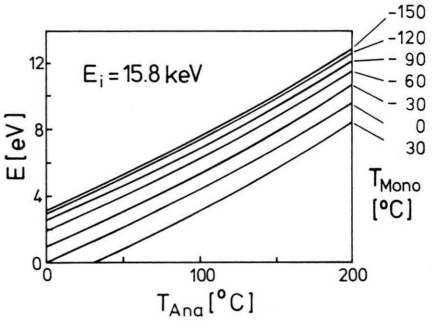

Fig. 4. Energy transfer as function of the analyzer temperature for a primary photon energy of 15.8 keV at different monochromator temperatures (from [15]).

The range of energy transfers accessible at the instrument INELAX is not limited to meV. The limits of a possible energy transfer are determined by the maximum temperature difference between monochromator and analyzer. Therefore, an increase of the energy transfer can be achieved by cooling the monochromator crystal. Figure 4 demonstrates an achievable range of 12 eV, using a primary photon energy of 15.8 keV and cooling the monochromator to low temperatures.

In the development of this instrument several applications were studied in different stages of the energy resolution. Longitudinal and transverse phonon dispersion curves could be determined in beryllium [7] and diamond [4]. Figure 5 shows the phonon dispersion curves in diamond in [00ξ] direction as measured with inelastic X-ray scattering. The observed frequencies drawn in an extended zone scheme are in good

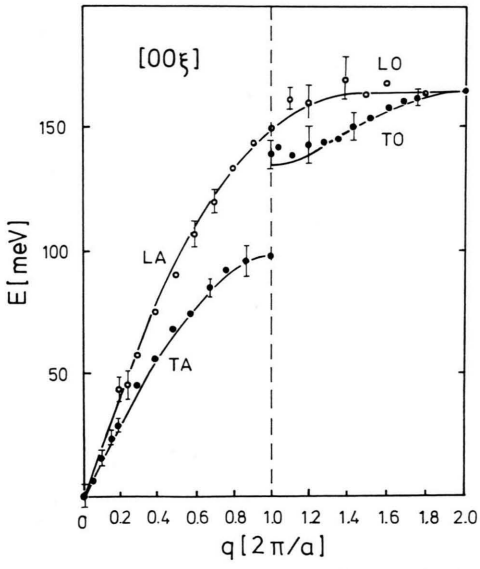

Fig. 5. Phonon dispersion curves for longitudinal (o) and transverse (●) modes in [00ξ] direction in diamond. In the extended zone scheme the Brillouin zone boundary is at $q = 1$.

agreement with a shell-model fit to neutron data from literature [8].

Inelastic scattering with high energy resolution has been to this point the domain of thermal neutron scattering. However, some research fields have opened now in which the new technique of inelastic scattering with X-rays can give valuable complementary information, not available with neutrons. Scattering experiments at small momentum transfers can be performed with X-rays at any desired energy transfer in contrast to neutron scattering experiments, where the velocity of the incoming neutrons has to be larger than the velocity of the sound in the sample material for the detection of a phonon gain peak. This is an important range in the energy-momentum space for the determination of the frequency spectra for excitations in amorphous, polycrystalline and liquid materials. Studies with INELAX were performed, using polycrystalline lithium. In the first-Brillouin-zone longitudinal vibrational modes could be observed [3, 9].

For the investigations of liquids with inelastic X-ray scattering at INELAX liquid lithium was chosen. The experiments were started with a moderate energy resolution $\delta E = 27$ meV [9] and later continued with an improved value of $\delta E = 12$ meV [10]. Figure 6 shows the scattered X-ray intensity at a temperature of 600 K as a function of the temperature difference

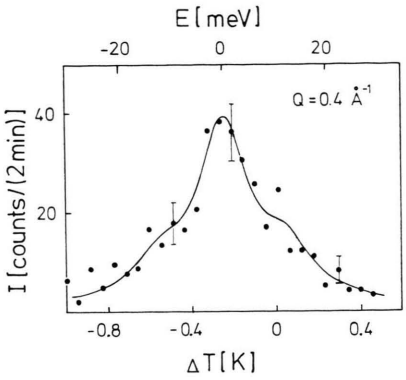

Fig. 6. X-ray intensity scattered from liquid lithium in a constant-$\boldsymbol{Q}$ scan at 0.4 $Å^{-1}$. The line represents a fit of three Lorentz curves with widths of 12 meV at half height.

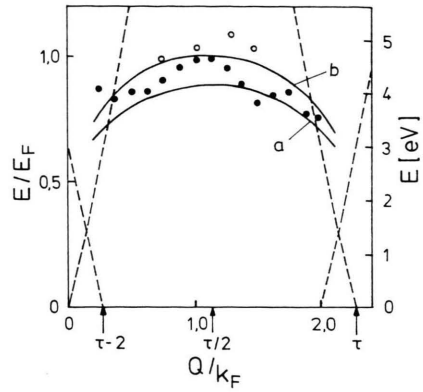

Fig. 8. Dispersion curve of the zone-boundary collective states in lithium in the [001] direction. For details see text.

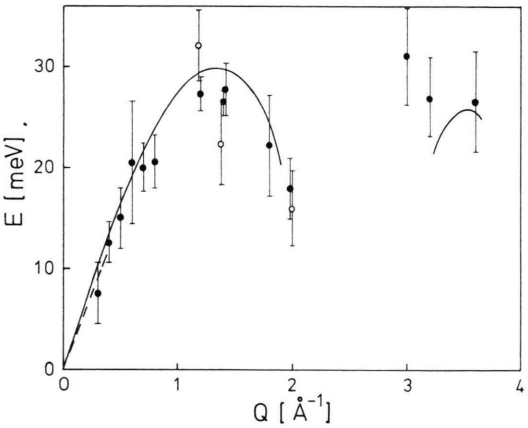

Fig. 7. Dispersion of the collective density modes in lithium at 600 K derived from the constant-$\boldsymbol{Q}$ scans in an E, Q diagram. (•) represent data obtained with improved energy resolution. The curve is calculated as discussed in the text. The dashed line represents a slope according to the adiabatic velocity of sound.

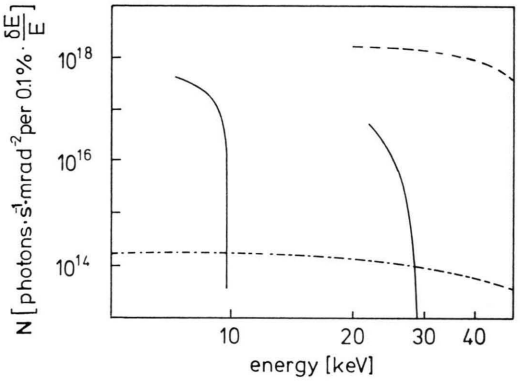

Fig. 9. The brightness as a function of energy for the HARWI wiggler (3rd harmonic, *solid line*) and for an undulator at PETRA, Hamburg (fundamental, *dashed line*).

and the corresponding energy transfer for a Q value of 0.4 $Å^{-1}$. This spectrum clearly demonstrates the expected excitation scheme of a quasielastic line with pronounced shoulders. The energy transfers, which could be derived for the collective density modes, are drawn in an energy-transfer–wavevector diagram in Fig. 7 and demonstrate the dispersion of these density modes. The adiabatic velocity of sound taken from [11] is shown as well. The position of the first maximum of the observed dispersion relation corresponds to $Q_0/2$, with Q_0 being the position of the first peak of the static structure factor of liquid lithium. In addition to the first maximum in $S(Q, \omega)$ there are indications for a second one at higher Q values. This means that the density modes are not overdamped in this Q region. The line drawn in Fig. 7 was calculated using a viscoelastic model, derived in [12, 13] for a monoatomic fluid, which includes fluctuations in the particle density and the energy density beyond the hydrodynamic limit. There is good agreement between the calculated curve and the X-ray data within the error bars. From the inelastic X-ray scattering data it is obvious that in the observed Q-range the liquid has a solid-state-like behavior with propagating waves. Around each atom

of the liquid a correlation region with a radius of several atomic distances can be expected. In this range collective coupled vibrations similar to phonons exist.

It is a challenging idea to apply the technique of inelastic X-ray scattering to even more complex systems than presented so far. As representatives of molecular crystals in the biological field, the crystallized amino acids glycine and alanine were chosen. Excitation energies of internal modes of these crystals could be observed as high as 400 meV. Their dispersions were also studied [3, 14].

Inelastic X-ray scattering is also an excellent tool to obtain information on valence-electron dynamics. The influence of the crystal lattice leads to zone-boundary collective states in metals like lithium. These are excitations that lie in the energy interval that is accessible with the instrument INELAX. The excitations were investigated with an energy resolution of 38 meV [3, 5, 15] compared to earlier performed experiments [16]. The dispersion curve of the zone-boundary collective states in lithium in [001] direction derived from INELAX data is shown in Figure 8. The broken lines give the range of intraband transitions of a free-electron gas in a weak lattice potential. The results are compared with the experimental results of [16]. The calculated dispersion curves of the zone-boundary collective states are shown according to [17] with the parameters for (a) taken from [18] and for (b) from [19]. The results of the experiments with INELAX clearly reveal fine structure of these collective states.

The increased resolution in inelastic X-ray scattering can be used to study the fine structure of the collective electron excitation states and to perform complementary studies to electron scattering. The latter is a powerful experimental tool for small momentum transfers Q, because of the dependence on Q^{-2}. At higher Q-values the scattering intensity is strongly decreasing, and, in addition, various multiple scattering processes are excited, thus making the interpretation of data tedious. In contrast, the X-ray scattering intensity is strongly increasing for higher Q values, since there is a dependence on Q^2 here. Moreover, no unwanted process occurs. Another important point is that, owing to strong absorption, electron scattering can only be performed in thin films. Therefore, inelastic X-ray scattering is not only complementary to electron-energy-loss spectroscopy, but opens new application fields.

The instrument INELAX brought a breakthrough in X-ray diffraction with the direct measurement of small energy shifts of photons. This step opened a wide field of research activities in high-energy-resolution work. Convincing results in single-crystal phonon scattering were obtained, demonstrating the power of the method. Experiments with polycrystalline and liquid matter show the competitive power of X-rays compared to neutrons. This is underlined by the detection of molecular vibrations in small biological samples. Investigations of electronic excitations with increased resolution reveal fine structure, demanding modified approaches in the theoretical discussion in this field. The attractiveness of inelastic X-ray scattering with high resolution and the ease of handling it is increased with higher photon fluxes at the sample. New synchrotrons being presently built will deliver such high fluxes. This is demonstrated by Fig. 9, which shows the brightness of different photon beams as a function of the energy. It compares the currently used HARWI wiggler at DORIS, Hamburg, with a projected symmetric undulator device at the ESRF, Grenoble, and with a study of an undulator device at PETRA, Hamburg. For details of this comparison see [3]. The brightness of a typical ESRF undulator is shown for the fundamental and the third harmonic. For the PETRA undulator only the fundamental is shown.

The instrument INELAX at an undulator at the ESRF or at the high-energy ring PETRA, Hamburg, will certainly make high-resolution experiments a phantastic method in X-ray diffraction and thus increase the number of applications.

The steady support of HASYLAB is appreciated very much. This project is supported by the Bundesministerium für Forschung und Technologie under the project number 03PE1LMU2.

[1] B. Dorner and J. Peisl, Nucl. Inst. Meth. **208,** 587 (1983).
[2] E. Burkel, J. Peisl, and B. Dorner, Europhys. Lett. **3,** 957 (1987).
[3] E. Burkel, Inelastic Scattering of X-Rays with Very High Energy Resolution, Springer Tracts in Modern Physics, Vol. **125,** Springer-Verlag, Berlin 1991.
[4] E. Burkel, B. Dorner, Th. Illini, and J. Peisl, Rev. Sci. Instrum. **60,** 1671 (1989).
[5] Th. Illini, E. Burkel, and J. Peisl, Jahresbereicht Hasylab 1989, Hamburg (1989).
[6] E. Burkel, B. Dorner, Th. Illini, and J. Peisl, J. Appl. Cryst., in press.
[7] B. Dorner, E. Burkel, Th. Illini, and J. Peisl, Z. Physik B. Condensed Matter **69,** 179 (1987).
[8] J. L. Warren, J. L. Yarnell, G. Dolling, and R. A. Cowley, Phys. Rev. **158,** 805 (1967).
[9] E. Burkel, S. Gaus, Th. Illini, and J. Peisl, PHONONS 89, Vol. **2,** 1436, World Scientific Publishing, 1990.
[10] H. Sinn and E. Burkel, Physica B, submitted.
[11] H. Ruppersberg and W. Speicher, Z. Naturforsch. **31a,** 47 (1976).
[12] S. W. Lovesey, J. Phys. C: Sol. State Phys. **4,** 3057 (1971).
[13] J. R. D. Copley and S. W. Lovesey, Rep. Prog. Phys. **38,** 461 (1975).
[14] M. Strohmeier, E. Burkel, and J. Peisl, Jahresbericht HASYLAB, Hamburg 1989.
[15] Th. Illini, Thesis, University Munich, 1991.
[16] W. Schülke, N. Nagasawa, S. Mourikis, and P. Lanzki, Phys. Rev. B **33,** 6744 (1986).
[17] K. Sturm and L. E. Oliveira, Europhys. Lett. **9,** 257; Phys. Rev. B **40,** 3672 (1989).
[18] W. Y. Ching and J. Callaway, Phys. Rev. B **9,** 5115 (1974).
[19] H. Bross and G. Bohn, Z. Phys. B **20,** 261 (1975).